# Laser Diffraction Determination of the Crystalline Structure of an Electrorheological Fluid

Tian-jie Chen,[a] R. N. Zitter, and R. Tao
*Physics Department, Southern Illinois University, Carbondale, Illinois 62901*
(Received 14 November 1991)

The electric-field-induced structures of small glass spheres in silicone oil produce laser diffraction patterns which verify, for the first time, the body-centered-tetragonal lattice structure predicted by theory. By a mechanism totally unlike that of conventional x-ray scattering, the incident laser beam propagates through the lattice of close-packed spheres via stable optic modes along regular arrays of transparent spheres, and then produces diffraction patterns after exiting from the lattice.

PACS numbers: 82.70.Gg, 61.16.−d, 61.90.+d

The electrorheological (ER) effect has attracted considerable attention recently [1–9]. An ER fluid, generally a suspension of small particles of high dielectric constant in a fluid of low dielectric constant, undergoes a transition to a gel-like state when an applied electric field exceeds a critical value [5]. Between the field electrodes, the particles first form chains which then coalesce into columns. Halsey and Toor [2] discussed the thermodynamics of the process and estimated that the columns have a width $\sim R(L/R)^{2/3}$, where $R$ is the radius of the dielectric particles and $L$ is the spacing between the two electrodes. Later, Tao and Sun [3] predicted that for uniform spherical particles the columns have a body-centered-tetragonal (bct) lattice structure, as illustrated in Fig. 1(a). The three conventional lattice vectors here are $\sqrt{6}R\hat{\mathbf{x}}$, $\sqrt{6}R\hat{\mathbf{y}}$, and $2R\hat{\mathbf{z}}$, with the field along the $z$ direction.

The prediction of a bct lattice as a many-body ground state of ER fluids has been confirmed by Monte Carlo simulations, which have also shown that this structure can be realized at room temperature [9]. However, there has been no experimental verification of the structure. Optical microscopic observations, such as those of Conrad, Fisher, and Sprecher [4], clearly showed the formation of chains and columns but the structure within columns was not apparent, and in any case, two-dimensional images at best only provide very limited information about three-dimensional structures. Since the electric-field-induced solidification in ER fluids is a relatively fast phase transition, it would be interesting to see if a regular lattice can be formed in the process. Furthermore, most existing theoretical models and calculations of ER fluid properties assume particles in chains rather than columns. Therefore, an experimental determination of column structure would be highly significant for future research and applications.

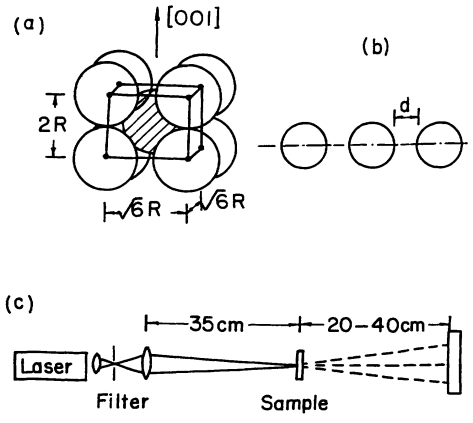


FIG. 1. (a) Unit cell of the bct lattice proposed by Tao and Sun for spheres of radius $R$, where the [001] axis is the applied field direction. (b) A linear periodic array of glass spheres of radius $R$ separated by a distance $d$. (c) Layout of the diffraction experiment. In the sample, whose view is given in Fig. 2(a), the applied electric field direction [001] is perpendicular to the optic axis.

In this Letter, we report an investigation of column structure by laser beam diffraction which confirms the predicted bct lattice structure. The diffraction mechanism, however, is totally unlike that of conventional x-ray scattering by crystals, and here we describe a new process for forming diffraction patterns by a close-packed lattice of transparent spheres.

Our ER fluid consists of a low-viscosity silicone oil containing size-selected glass microspheres of highly uniform diameter, either $20.0 \pm 1.8$ or $40.7 \pm 1.7$ $\mu$m (SPI Supplies, Westchester, PA). The glass spheres were pretreated [4,10] to develop an absorbed $H_2O$ film which greatly enhances their effective dielectric constant, and then the spheres were mixed with oil to a volume fraction of about 0.2. On a horizontal microscope glass slide we mounted two parallel brass electrodes which were 3 mm thick and separated by 3 mm. Then three glass spacers were used between the electrodes, one at the bottom and two at the two sides, to form an ER fluid cell in a region of the most uniform electric field. Only a small drop of the ER liquid is needed to fill the cell, measuring 3 mm × 3 mm horizontally and 0.3 mm in vertical depth. The top surface of the fluid is open (no cover glass is used). Before an electric field was applied, the spheres stayed at the bottom and formed several layers. We stirred the ER fluid in the cell first to make the spheres spread into the space, and then we began to apply an electric field. The solidi-

 

fication process takes about 5 min and is recorded by a video camcorder, showing the formation of chains and then columns for applied electric fields $\sim 1$ kV/mm. If the field is maintained for several hours, the oil leaks out of the cell and the structures become "locked" in place, remaining fixed after removal of the field. The average column width is 0.6 mm which is close to the theoretical prediction by Halsey and Toor [2]. The column thickness vertical to the slide is about 0.15 mm. The average separation between two columns is generally several column widths. We calculate that the buoyancy-corrected gravitational potential energy for a sphere to climb one layer up is smaller than the crystal formation energy in our ER fluid [3]. The dipole-dipole force between spheres within one horizontal layer in our ER fluid is at least 10 times stronger than gravitation. Therefore, sedimentation due to gravity (perpendicular to the microscope slide) may limit the vertical column thickness of our samples, but does not cause any problem for formation of lattice structure.

The diffraction of a laser beam by glass spheres in a closed-packed lattice such as that shown in Fig. 1(a) needs to be carefully examined. It certainly is *not* analogous to conventional x-ray diffraction by a crystal. For x rays, a crystal is essentially transparent with a three-dimensional array of small scattering centers (nuclei and electrons) that produce far-field interference patterns. In our ER structure, the glass spheres have a size much larger than the laser wavelength (0.63 $\mu$m), and the closely packed structure is "optically dense" in the sense that there are very few paths for light to travel without encountering a number of spheres. In fact, for example, there is no direct path in the [110] direction. Although one might expect diffuse scattering of a laser beam due to multiple reflections and refractions by the spheres, a mechanism for producing regular patterns is not immediately obvious.

We propose the following process. Since each glass sphere acts as a "thick" lens, a linear periodically spaced set of spheres, as shown in Fig. 1(b), constitutes a periodic array of focusing elements. An analysis of such arrays can be found in many texts [11], where it is shown that light rays can propagate stably and indefinitely along an appropriately spaced set of such elements. In other words, there are stable ray modes that do not diverge from the axis, or leave the array. This analysis is often employed in laser design, where an infinite array is used to represent the end reflectors of an optical cavity [11]. Mathematically, the path of a ray along a single periodic length is characterized by a $2\times 2$ matrix $M$, and stable ray modes exist if the absolute value of the trace of $M$ is less than 2.

The calculation of $M$ is simple for "paraxial" rays close to the array axis that make only small angles from the axis. For the array represented in Fig. 1(b), the matrix for the period from the front surface of one sphere to the front surface of the next is given by

$$M=\begin{pmatrix}1 & d\\ 0 & 1\end{pmatrix}\begin{pmatrix}1 & 0\\ (1-n)/R & n\end{pmatrix}\begin{pmatrix}1 & 2R\\ 0 & 1\end{pmatrix}\begin{pmatrix}1 & 0\\ (1-n)/nR & 1/n\end{pmatrix}=\begin{pmatrix}[(2-n)/n]+[2d(1-n)/nR] & [2R/n]+[d(2-n)/n]\\ 2(1-n)/nR & (2-n)/n\end{pmatrix}, \quad (1)$$

where $R$ is the radius, $n$ is the ratio of the refractive index of the spheres to the refractive index of air medium, and the matrices in the product, reading from right to left, represent respectively (i) refraction entering a sphere, (ii) traverse through the sphere, (iii) refraction leaving the sphere, and (iv) traverse of the space $d$ between two spheres. Each of these matrices can be found in the ray-matrix tables of Ref. [11]. For stable ray modes, the absolute value of the trace of $M$ must be less than 2. Then, from Eq. (1), we obtain the stability condition

$$d<2R/(n-1). \quad (2)$$

Our samples, after the oil leaks out, have $n=n_{\text{glass}}/n_{\text{air}}=1.51$ and thus we require $d<3.9R$ for stable mode propagation. For the bct lattice shown in Fig. 1(a), all directions $[m,n,l]$ with low indices $(m,n,l=0,\pm 1)$ satisfy the above condition, and accordingly, stable paraxial ray modes may propagate along these directions. More extensive calculations show that stable nonparaxial modes may also propagate in the bct lattice.

Thus, stable modes travel along each linear array and emerge from the final sphere to a focus beyond the last lattice plane. The focal waist size is only a few micrometers in diameter, small in comparison with the sphere radius. The set of such focal "points" is essentially a two-dimensional array (not three dimensional as with x rays) that produces a diffraction pattern. Therefore, the form of the far-field diffraction pattern is just the reciprocal lattice of the exit plane. More specifically, diffraction maxima occur when

$$\mathbf{k}\cdot(l\mathbf{a}+m\mathbf{b})=2N\pi, \quad (3)$$

where $\mathbf{k}$ is a diffracted wave vector, $\mathbf{a}$ and $\mathbf{b}$ are the lattice vectors in the exit plane, and $l$, $m$, and $N$ are integers. The solutions of $\mathbf{k}$ which satisfy Eq. (3) are just the reciprocal lattice vectors of the exit plane. In short, the optical output of the glass spheres lattice is a two-dimensional set of bright focal spots that produce the far-field pattern.

The experimental optical diffraction arrangement is shown in Fig. 1(c). A 5-mW He-Ne laser beam is passed through a spatial pinhole filter to obtain a clean Gaussian intensity profile and is then focused onto an individual column of the sample. The focused laser beam has a Gaussian diameter about 0.1 mm or $\frac{1}{6}$ of the average column width. The sample is on a micrometer adjustable mount for translation and angular rotation. We note a

fundamental difference between our experiment and conventional x-ray diffraction by a crystal. In the latter case, the Bragg condition requires a specific orientation of the incident beam relative to crystal planes, and all orientations must be used to obtained a complete pattern. By contrast, our experiment is insensitive to the incident beam direction and an entire planar pattern for the lattice exit plane is obtained for a single orientation of the sample relative to the incident beam. This is because each sphere in the first layer encountered by the beam produces refracted rays in various directions, from which propagating array modes are selected by deeper-lying layers.

Figure 2(a) is a microscopic view of typical columns. In a situation similar to Ref. [4], regardless of magnification, we are unable to discern the crystalline structure within the columns in two-dimensional images with certitude; therefore, we examine the diffraction patterns obtained, e.g., Figs. 2(b)–2(d). The bct lattice structure proposed by Tao and Sun [3] can be identified by the structures of the (110) and (100) planes. The (100) plane has a rectangle $\sqrt{6}R\times 2R$ as a primitive cell, while the (110) plane is a centered rectangular lattice of $2\sqrt{3}R\times 2R$. Figure 2(b) shows a diffraction pattern produced by a sample with 20.0-$\mu$m-diam spheres. The geometry of this pattern is precisely the reciprocal lattice of the (110) plane in the bct structure and the structure constants derived from the pattern are precisely those expected for this plane. This implies that the transmission axis of stable ray modes is along the axis [110]. Figure 2(c) shows a pattern from a sample with 40.7-$\mu$m-diam spheres. Here the pattern is also that of a reciprocal lattice of the (110) plane, but twice as dense as in Fig. 2(b) because with spheres twice as large the reciprocal spacing is smaller by $\frac{1}{2}$. In Fig. 2(d), the sphere diameter is 40.7 $\mu$m and the pattern is obviously more rectangular than in the preceding cases; it is, in fact, precisely the pattern expected for a (100) plane. In this case, the transmission axis of stable ray modes is [100]. The direction [010] is equivalent to [100] in the bct structure. All of our samples have shown diffraction patterns consistent with the bct lattice structure.

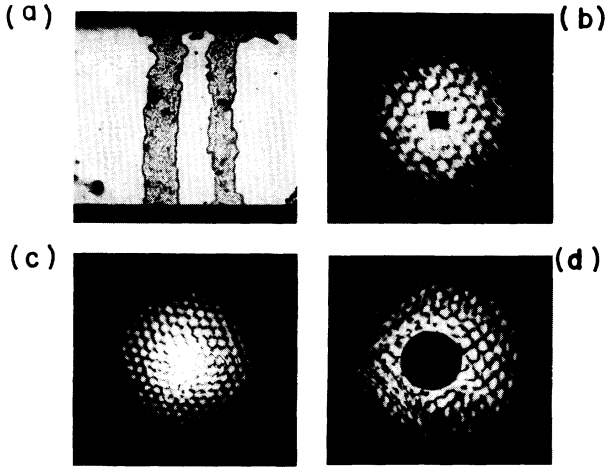


FIG. 2. (a) View of typical columns formed between the two electrodes which are separated by 3 mm. (b) Diffraction pattern of a (110) plane for 20.0-$\mu$m-diam spheres. (c) Pattern of a (110) plane for 40.7-$\mu$m-diam spheres. (d) Pattern of a (100) plane for 40.7-$\mu$m-diam spheres. In (b) and (d), the centers are masked to suppress overexposure.

We have also extensively searched in our samples for any other lattice structures, such as face-centered-cubic (fcc) and body-centered-cubic (bcc) lattices. If there is a fcc lattice structure, there should be a square lattice plane of $2R\times 2R$ and a rectangular lattice plane of $2R\times\sqrt{8}R$ which distinguish the fcc lattice from the bct lattice. We have not found any diffraction pattern consistent with the fcc lattice structure. If there is a bcc structure, we should see two lattice planes, a square lattice of $(4/\sqrt{3})R\times(4/\sqrt{3})R$ and a centered rectangular lattice of $(4/\sqrt{3})R\times 4\sqrt{2/3}R$. We have not found any such structures either. Therefore, there are no fcc or bcc lattice structures in our samples.

Table I lists experimental results of the structure constants compared with theoretical values for the bct lattice. In all cases, there is agreement to within a few percent. As mentioned earlier, the diameters of our spheres are known to be nonuniform to this degree. Accordingly, the data are entirely consistent with the proposed bct lattice.

As mentioned earlier, column dimensions perpendicular to the electric field are 0.6 mm×0.15 mm. For a bct lattice of 20-$\mu$m-diam spheres, this represents 50×12 lattice layers. With the small size of our laser beam focus, we can probe the structure at different points of a column, and the bct lattice (100) or (110) patterns noted above are observed at different locations along a given column. Thus the overall column structure can be described as "polycrystalline," with the provision that the [001] applied field axis is maintained.

Our sample geometry, in which columns are formed between brass electrodes on a glass slide, is well suited for microscopic observation of the columns as in Fig. 2(a) and for diffraction experiments with the laser beam perpendicular to the applied field direction (axis [001]). Clearly, the arrangement is not suitable for obtaining a

TABLE I. Structure constants.

| Lattice plane | Sphere diameter ($\mu$m) | Experiment ($\mu$m) | Theory ($\mu$m) |
|---|---|---|---|
| (110) | 20.0 | $a=34.1$ | 34.6 |
| | | $b=21.1$ | 20.0 |
| (110) | 40.7 | $a=69.1$ | 70.5 |
| | | $b=38.9$ | 40.7 |
| (100) | 40.7 | $a=54.8$ | 49.8 |
| | | $b=43.8$ | 40.7 |

(001) pattern, which would require a beam along the [001] direction, tangential to the slide and penetrating the electrodes.

This work is supported by Office of Naval Research Grant No. N00014-90-J-4041. We wish to thank Dr. Xuesong Zhang for valuable assistance.

---

[a]On leave from Physics Department, Peking University, Beijing, China, 100871.

[1] For a recent overview see, *Electrorheological Fluids*, edited by J. D. Carlson, A. F. Sprecher, and H. Conrad (Technomic Publishing, Lancaster, PA, 1990).

[2] T. C. Halsey and W. Toor, Phys. Rev. Lett. **65**, 2820 (1990).

[3] R. Tao and J. M. Sun, Phys. Rev. Lett. **67**, 398 (1991).

[4] H. Conrad, M. Fisher, and A. F. Sprecher, in *Electrorheological Fluids* (Ref. [1]), p. 63.

[5] R. Tao, J. T. Woestman, and N. K. Jaggi, Appl. Phys. Lett. **55**, 1844 (1989).

[6] H. Block and J. P. Kelly, U.S. Patent No. 4687589 (1987); J. D. Carlson, U.S. Patent No. 4772407 (1988); F. E. Filisko and W. E. Armstrong, U.S. Patent No. 4744914 (1988).

[7] D. J. Klingenberg, F. van Swol, and C. F. Zukoski, J. Chem. Phys. **91**, 7888 (1989).

[8] G. Bossis and J. F. Brady, J. Chem. Phys. **91**, 1866 (1989).

[9] R. Tao and J. M. Sun, Phys. Rev. A **44**, R6181 (1991).

[10] L. Hollan, *The Properties of Glass Surfaces* (Wiley, New York, 1964).

[11] See, for example, A. E. Siegman, *Lasers* (University Science Books, Mill Valley, CA, 1986), Chap. 15.

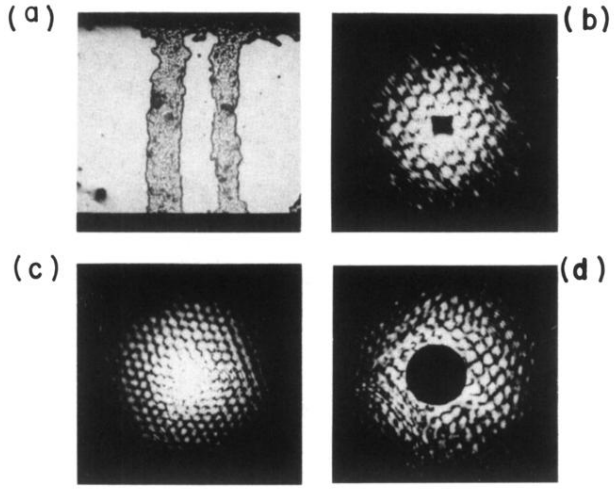


FIG. 2. (a) View of typical columns formed between the two electrodes which are separated by 3 mm. (b) Diffraction pattern of a (110) plane for 20.0-$\mu$m-diam spheres. (c) Pattern of a (110) plane for 40.7-$\mu$m-diam spheres. (d) Pattern of a (100) plane for 40.7-$\mu$m-diam spheres. In (b) and (d), the centers are masked to suppress overexposure.